

## Clinical report

# Magnetic resonance imaging findings of hepatocellular carcinoma: typical and atypical findings

Laddawan Vajragupta, Khanitha Kittisatra, Kewalee Sasiwimonphan

Department of Radiology, Faculty of Medicine, Chulalongkorn University, Bangkok 10330, Thailand

**Background:** Hepatocellular carcinoma (HCC) is the most common primary liver malignancy. Magnetic resonance imaging has been widely used for detection and characterization of HCC.

**Objective:** Describe MRI findings of HCC and to define the typical and atypical appearances of HCC on magnetic resonance images.

**Methods:** We retrospectively reviewed MRI findings of 100 HCC in 78 patients. Diagnosis was confirmed by angiography, pathology or follow up imaging. The signal intensity, size, margins, enhancement pattern, and other features were evaluated. Imaging findings between small HCC ( $\leq 2$  cm) and large HCC ( $>2$  cm) were compared.

**Results:** The most common signal intensity of HCC on unenhanced T1- and T2-weighted images was hypointense on T1-weighted images and hyperintense on T2-weighted images (65%). Most HCC (91%) were hyperintense on T2-weighted images. Isointensity on T2-weighted images were found in 9% of HCC. The typical enhancement pattern of HCC was enhancement on the arterial phase and washout on the portovenous phase (84%). Atypical enhancement pattern of HCC were enhancement on the portovenous phase in 5%, rim enhancement on the arterial phase or portovenous phase were demonstrated in 2%. Hyperintensity of the tumor on delayed phase was found in 19%. There was no statistically significant difference in signal intensity, enhancement, and washout pattern between small and large HCC. Fatty metamorphosis, mosaic pattern, necrosis, capsule and vascular involvement were found in 18%, 42%, 5%, 62%, and 6%, respectively. Mosaic pattern, necrosis, capsule, and vascular involvement were observed more frequently in large HCC.

**Conclusion:** The typical appearance of HCC was hypointense on T1-weighted, hyperintense on T2-weighted images, arterial enhancement and portovenous washout. Atypical appearances of HCC were rim enhancement on the arterial phase or portovenous phase and persistent enhancement on the delayed phase.

**Keywords:** Capsule, fatty metamorphosis, hepatocellular carcinoma, magnetic resonance imaging, mosaic pattern, necrosis

Hepatocellular carcinoma (HCC) is the most common primary malignant tumor of the liver. The prevalence of HCC is high in Africa and Asia including Thailand. The primary causative factors in high-incidence areas are hepatitis B and C virus infection [1].

Magnetic resonance imaging (MRI) is very useful in differentiation of hepatic nodules. In cirrhotic liver, MRI plays a major role in differentiation of regenerative nodules, dysplastic nodules, and HCC

[2]. In comparison with computed tomography, MRI provides better soft tissue contrast and provides greater sensitivity for lesion detection [3-5]. Early detection of HCC helps improve patient survival by allowing prompt treatment including partial hepatectomy, liver transplantation, radiofrequency ablation, percutaneous ethanol injection, and transarterial chemoembolization. The five-year survival rate for the patients with HCC has been improved [6].

Typical imaging appearance of HCC is arterial hypervascularity and washout on the early or delayed venous phase. According to the American Association for the Study of Liver Diseases (AASLD) practice guideline [6], if serum  $\alpha$ -fetoprotein is greater than

**Correspondence to:** Assoc Prof. Laddawan Vajragupta, Department of Radiology, Faculty of Medicine, Chulalongkorn University, Bangkok, 10330, Thailand. Email: vajragupta\_l@yahoo.com

200 ng/mL and the radiological appearance of the mass is suggestive of HCC (mass larger than 2 cm with arterial hypervascularity and washout in the venous phase), the likelihood that the lesion is HCC is high, and biopsy is not essential.

The purpose of our study was to describe MRI findings of HCC and to define the typical and atypical appearances of HCC on MR images. Different findings between small and large HCC was analyzed.

## Materials and methods

### *Patient population*

Between January 2006 and December 2008, patients with 100 HCC in King Chulalongkorn Memorial Hospital were enrolled. This study was approved by the Ethics Committee of the Faculty of Medicine, Chulalongkorn University.

The inclusion criteria were as follows: 1) patients with known or suspected of having newly developed HCC, and 2) confirmation of HCC by at least one of the following criteria: i) biopsy or surgical resection proven of HCC, and ii) serum  $\alpha$ -fetoprotein greater than 200 ng/mL and/or typical HCC findings on angiography (tumor staining, hypervascularity, or neovascularity on the arterial phase with washout on the portovenous phase) and/or increased size of lesion in follow-up imaging.

In cases of multifocal newly developed lesions, we included only the lesions that showed typical HCC findings on angiography or increased size in follow-up imaging.

The exclusion criteria were as follows: a) history of prior therapy for HCC in the studied lesion including surgery, transarterial chemoembolization, radiofrequency ablation, or percutaneous ethanol injection, or b) no confirmation of HCC.

There were 77 male and 23 female patients aged 40-85 years (means  $63.5 \pm 10.2$  years).

### *Magnetic resonance (MR) imaging technique*

All MR imaging were performed with a 1.5-T system (Signa, GE Medical Systems, Milwaukee, USA).

The imaging protocol included T1-weighted images acquired as fast spoiled gradient-echo sequences both in-phase and out-of-phase (repetition time/echo time msec, 60-165/4.0-4.3 for in-phase and 60-165/2.0-2.3 for out-of-phase), flip angle  $80^\circ$ , field of view (FOV) 30-38 x 30-38 cm, matrix 256 x 192, 8-mm-thick sections with a 1-mm intersection gap.

T2-weighted fat-suppressed fast spin echo sequence was acquired with TR/TE range of 6000-9300/90-100 msec, FOV 30-38 x 30-38 cm, matrix 320 x 224, 8-mm-thick sections with a 1-mm intersection gap.

Gadolinium was administered as an intravenous bolus in dosage of 0.1 mmol/kg. Fat saturated T1-weighted three-dimensional fast spoiled gradient-echo sequences were performed before and after administration of gadolinium in the hepatic arterial phase (20-30 seconds after contrast injection), the portovenous phase (60 seconds after contrast injection), the equilibrium phase (90 seconds after contrast injection) and delayed phase at three minutes and 10-15 minutes after contrast injection.

In cases that superparamagnetic iron oxide (SPIO) was administered, 1.4 mL of SPIO was injected intravenously, then T2-weighted fat suppressed fast spin echo (TR/TE range of 7500-8000/95-100, FOV 30-38 x 30-38 cm, matrix 320 x 224, slice thickness 8 mm with a 1-mm intersection gap) and T2\* gradient echo sequences (140-165/8.6, flip angle  $20^\circ$ , FOV 30-38 x 30-38 cm, matrix 256 x 192, section thickness 7-8 mm with a one-mm intersection gap) were acquired additionally at 15 minutes and 20 minutes, respectively.

### *MRI findings analysis*

MR images were reviewed retrospectively in Picture Archiving and Communication System (PACS) by two radiologists independently. Differences among the observers were resolved by consensus.

Size of focal liver lesion was measured in two-dimensions in axial images, and the maximum one was collected. Size of lesions were categorized as small if the diameter was smaller than or equal to 2 cm or large if the diameter was larger than 2 cm.

Signal intensity of the lesion in each sequence was classified as hypointense, isointense, or hyperintense, compared to the surrounding liver parenchyma. Enhancement patterns were evaluated on the arterial, portovenous, equilibrium and delayed three-minute phases, and classified as hypointense, isointense, or hyperintense, compared to the surrounding liver parenchyma. When lesions showed heterogeneous signal intensity on T1-weighted, T2-weighted, or any phases of post contrast study, they were categorized as hypointense, isointense, or hyperintense according to predominant parts of the lesions. Phase of enhancement was defined as the phase that showed obvious increased signal intensity of the lesion after contrast media administration. Phase of washout

was defined as the phase that showed significant decreased signal intensity of the lesion after enhancement. On the delayed phase, rim enhancement of tumor capsule was also reviewed.

Presence of fatty change in tumors, mosaic pattern, necrosis, tumor capsule, and vascular involvement, including nodule within nodule appearance, were also evaluated.

Intracellular fatty change was defined as drop signal intensity area in tumors on out-of-phase images comparing with in-phase images. Mosaic pattern was defined as non-uniform signal intensity on T2-weighted images or multiple nodular enhancing areas on post contrast study [7, 8].

Central tumor areas with hypointensity on T1-weighted images, hyperintensity on T2-weighted images and no contrast enhancement were evaluated as necrosis. Capsule was rim of the tissue surrounding tumor with hypointense on T1- and T2-weighted images. Contrast enhancement of capsule was also recorded.

Nodule within nodule appearance was defined as a focus of high signal intensity within a low signal intensity nodule on T2-weighted images with enhancing focus on arterial phase [9].

Vascular involvement was defined as non-visualization or encasement of the venous structures in portovenous phase.

### Statistical analysis

Statistical analysis was performed using SPSS version 11.5. Continuous variables were expressed as mean±SD. Difference in appearance between tumors of less than or equal to 2 cm and those of

greater than 2 cm were tested using the Chi-square analysis.

### Results

There were 100 lesions in 78 patients in this study. Sixty four lesions located in right hepatic lobe, 35 lesions located in left hepatic lobe and one lesion located in both right and left hepatic lobes. Most lesions, 75 out of 100 (75%), were confirmed to be HCC by typical appearance on angiography. There were pathological confirmations in 16 lesions (16%): seven by FNA, four by core biopsy, and five by surgery. Grading of 16 pathological proven HCC were classified in well-differentiated in five lesions, moderately differentiated in three lesions, poorly-differentiated in three lesions, and unclassified in five lesions. Confirmation by increased size on follow-up imaging was considered in nine lesions (9%). Tumor sizes ranged from 0.7 cm to 16.7cm (means 3.1±2.98 cm). Forty-four lesions were smaller than 2 cm (44%) and 56 lesions were larger than 2 cm (56%).

On T1-weighted images, 67 lesions were hypointense (67%), 10 were isointense (10%), and 23 were hyperintense (23%). On T2-weighted images, 91 lesions were hyperintense (91%), and 9 were isointense (9%). **Table 1** summarizes data on signal intensity of HCC on un-enhanced T1- and T2-weighted images.

The typical signal intensity of HCC on un-enhanced T1- and T2-weighted images was hypointense on T1-weighted and hyperintense on T2-weighted (65%) (**Fig. 1**), followed by hyperintense on T1-weighted images and hyperintense on T2-weighted images (16%) (**Fig. 2**) and isointense on T1-weighted images and hyperintense on T2-weighted images (10%).

**Table 1.** MR imaging findings of HCC on T1-weighted and T2-weighted images.

Signal intensity T1-weighted images	T2-weighted images	Number of lesions
Hypointense	Hypointense	0
Hypointense	Isointense	2
Hypointense	Hyperintense	65
Isointense	Hypointense	0
Isointense	Isointense	0
Isointense	Hyperintense	10
Hyperintense	Isointense	7
Hyperintense	Hyperintense	16
Total		100

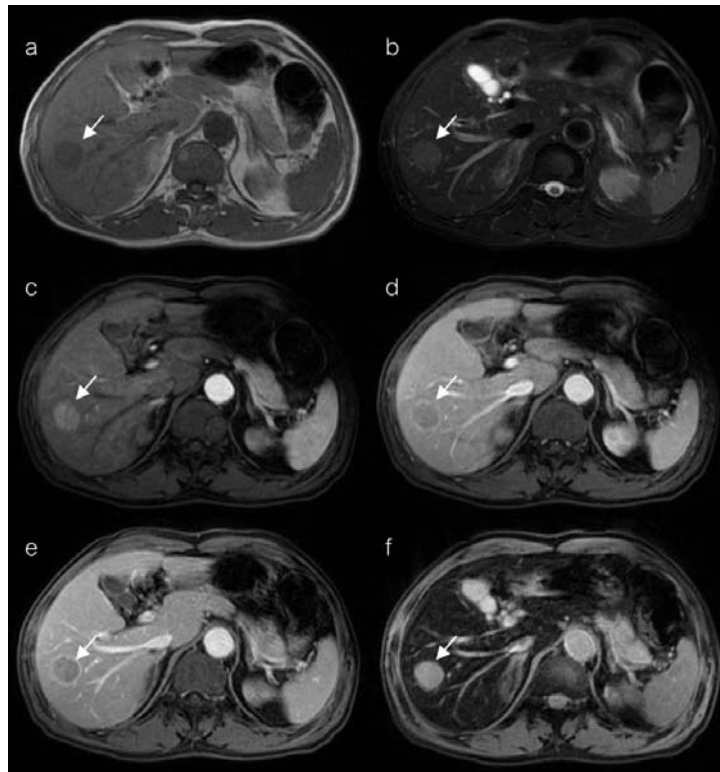


**Fig. 1** A 69-year-old man had a 2.7 cm moderately differentiated HCC in the right hepatic lobe (indicated by arrows). The lesion was hypointense on T1-weighted (a) and hyperintense on T2-weighted images (b). Arterial enhancement (c) and washout on the portovenous phase (d) with capsule enhancement on the delayed phase (e) were observed. This lesion showed no superparamagnetic iron oxide (SPIO) uptake on gradient echo T2\*-weighted image (f).

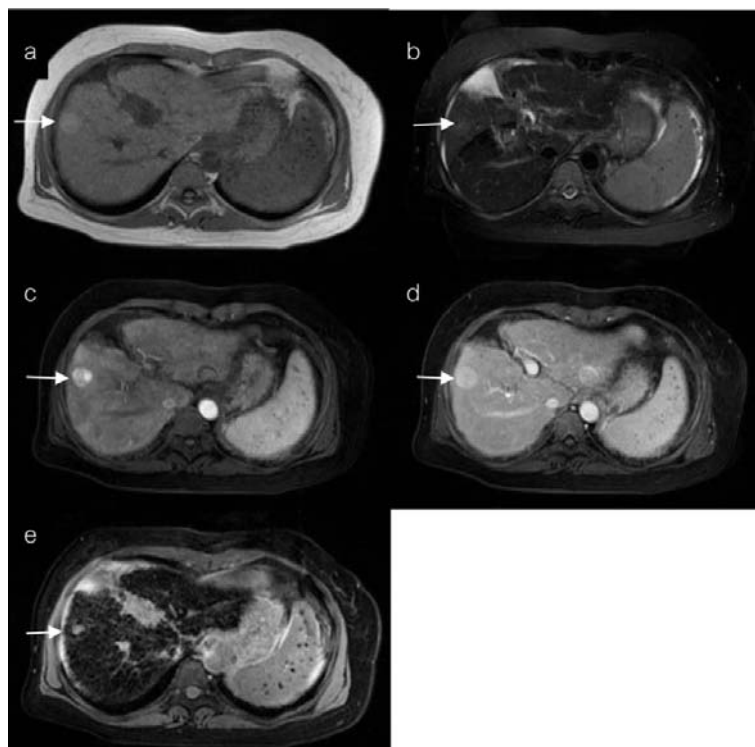


**Fig. 2** A 52-year-old woman had 2.3 cm well-differentiated HCC in the right hepatic lobe (indicated by arrows). The lesion was hyperintense on T1-weighted (a), mildly hyperintense on T2-weighted images (b), enhanced on the arterial phase with mosaic pattern (c), relative washout on the portovenous phase (d). Partial uptake of SPIO on gradient echo T2\*-weighted image was seen (e).

Among 44 HCC that were smaller than or equal to 2 cm, 29 lesions were hypointense (65.9%), seven were isointense (15.9%), and eight were hyperintense (18.2%) on T1-weighted images. On T2-weighted images, five were isointense (11.4%) (Fig. 3) and 39 were hyperintense (88.6%). Among 56 HCC that were larger than 2 cm, 38 lesions were hypointense (67.8%), three were isointense (5.4%), and 15 were hyperintense (26.8%) on T1-weighted images. On T2-weighted images, five were isointense (7.1%) and 52 were hyperintense (92.9%). There was no statistically significant difference in signal intensity of the tumors on T1-weighted and T2-weighted images between small ( $\leq 2$  cm) and large HCC ( $> 2$ cm) ( $p > 0.05$ ).

Ninety-five lesions demonstrated enhancement on arterial phase and five lesions demonstrated enhancement on portovenous phase. Among 95 lesions that enhanced on arterial phase, 84 lesions washed out on portovenous phase (see Fig. 1), nine lesions washed out on equilibrium phase and two lesions washed out on delayed phase. Among the five lesions that enhanced on portovenous phase, three lesions washed out on equilibrium phase, and two lesions washed out on delayed phase (Fig. 4). Table 2 shows phase of enhancement and phase of washout of HCC.

Signal intensity of the lesions on the delayed phase was hypointense in 71%, hyperintense in 19% (see Fig. 4), and isointense in 10%.

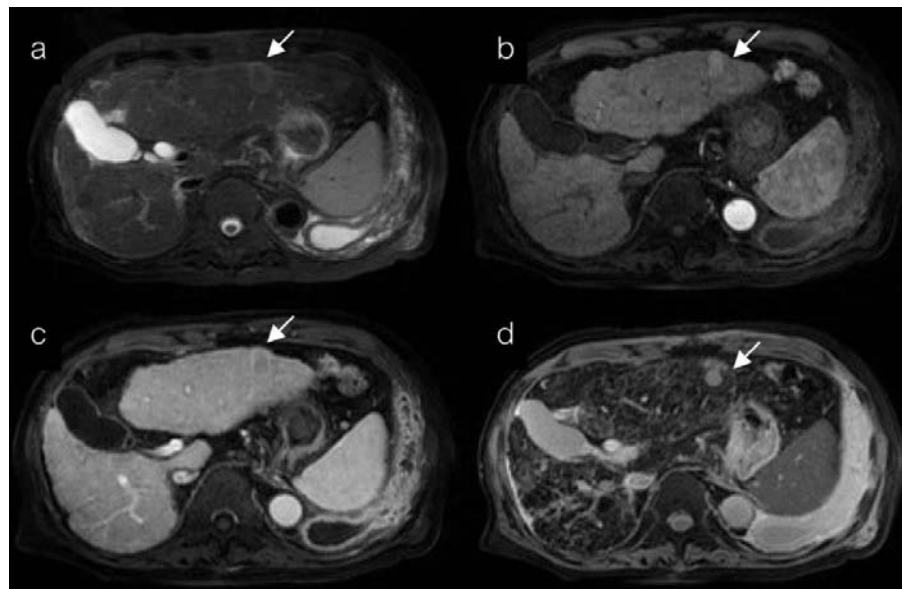


**Fig. 3** A 75-year-old man had a 1.8 cm HCC in the left hepatic lobe (indicated by arrows). The lesion was isointense with hyperintense rim on T2-weighted image (a). Enhancement on the arterial phase (b) and washout on the portovenous phase (c) were seen. The lesion did not uptake SPIO on gradient echo T2\*-weighted image (d).

**Table 2.** Enhancement pattern on MR imaging of HCC.

Enhancement	Washout	Number of lesions
Arterial phase	Portovenous phase	84
Arterial phase	Equilibrium phase	9
Arterial phase	Delayed phase	2
Portovenous phase	Equilibrium phase	3
Portovenous phase	Delayed phase	2
Total		100

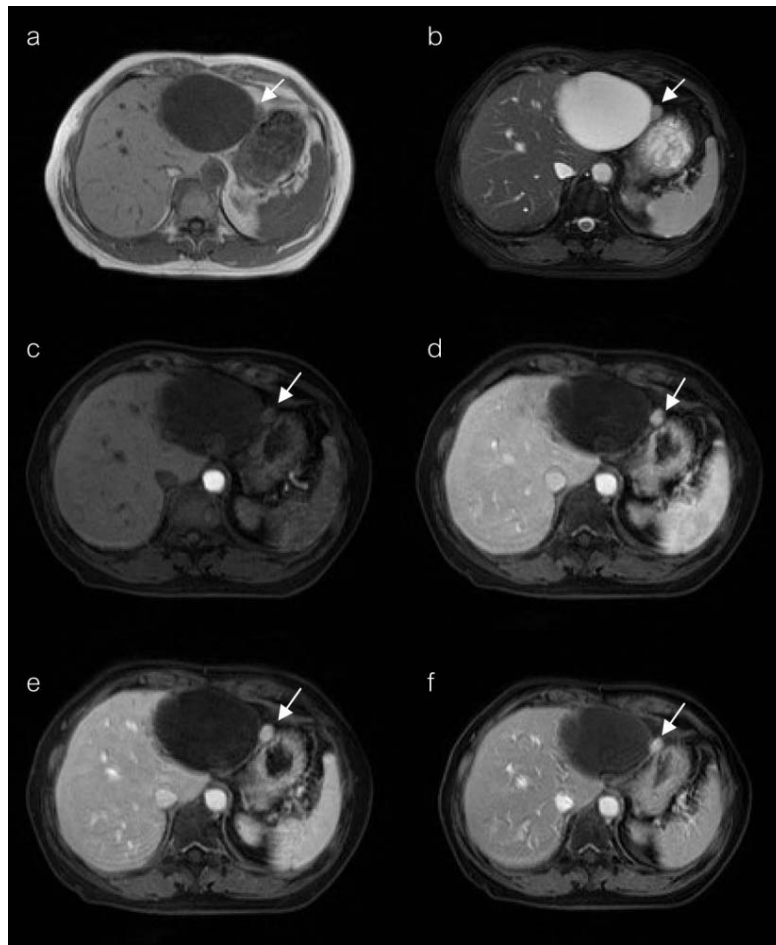


**Fig. 4** A 73-year-old woman had a 1.1 cm HCC in the left hepatic lobe (indicated by arrows) adjacent to the large hepatic cyst. This lesion was hypointense on T1-weighted (**a**) and mildly hyperintense on T2-weighted images (**b**). There was minimal enhancement on the arterial phase (**c**), intense enhancement on the portovenous phase (**d**) and equilibrium phase (**e**) with partial washout on the delayed phase (**f**).

Rim enhancement pattern was found in two lesions, one on the arterial phase (**Fig. 5**) and one on the portovenous phase (**Fig. 6**). Nodule within a nodule pattern was seen in three lesions in two patients (**Fig. 7**).

Among 44 HCC that were smaller than or equal 2 cm, 38 lesions (86.3%) were enhanced on the arterial phase and washout on the portovenous phase, four lesions (9.1%) were enhanced on the arterial phase and washout on the equilibrium phase, one lesion (2.3%) was enhanced on the portovenous phase and washout on the equilibrium phase, and one lesion (2.3%) was enhanced on the portovenous phase and washout on the delayed phase. Among 56 HCC that were larger than 2 cm, 46 lesions (82.1%) were enhanced on the arterial phase and washout on the portovenous phase, five lesions (8.9%) were enhanced

on the arterial phase and washout on the equilibrium phase, two lesions (3.6%) were enhanced on the arterial phase, and washout on the delayed phase, two lesions (3.6%) were enhanced on the portovenous phase and washout on the equilibrium phase, and one lesion (1.8%) was enhanced on the portovenous phase and washout on the delayed phase. There was no statistically significant difference in enhancement and washout pattern between small ( $\leq 2$  cm) and large HCC ( $> 2$  cm) ( $p > 0.05$ ).

Fatty metamorphosis was identified in 18 lesions (18%) (**Fig. 8**), including 11 out of the 56 HCC larger than 2 cm and seven out of the 44 HCC smaller than or equal 2 cm. Mosaic pattern was detected in 42 lesions (42%) (see **Fig. 2**), including 37 out of the 56 HCC larger than 2 cm and five out of the 44 HCC smaller than or equal 2 cm. Necrosis was found in

five lesions (5%) (**Fig. 9**), all of them are more than 2 cm in size. Capsules were identified in 62 lesions (62%) (**Fig. 9**), including 46 out of the 56 HCC larger than 2 cm and 16 out of the 44 HCC smaller than or equal 2 cm. Vascular involvement was observed in six lesions (6%), all of them are larger than 2 cm (**Fig. 10**). Mosaic pattern, necrosis, capsule, and vascular involvement were observed more frequently in large HCC. There was no statistically significant difference in fatty metamorphosis between small ( $\leq 2$  cm) and large HCC ( $> 2$ cm) ( $p > 0.05$ ).

SPIO was administered in 71 lesions in 57 patients. Sixty-six lesions (93%) showed no uptake (see **Fig. 1**) and five lesions (7%) showed partial uptake (see **Fig. 2**).

### Discussion

On MR images, HCC has variable signal intensity on T1-weighted images. HCC is usually hypointense on T1-weighted images, but hyperintensity are common. Hyperintensity on T1-weighted images are related with fatty metamorphosis, hemorrhage, copper-binding protein and glycogen [10]. On T2-weighted images, HCC are often hyperintense, contrast to the cirrhotic nodules that usually isointense or hypointense

to the liver. However, some HCC have similar signal characteristics to cirrhotic nodules.

Kelekis et al. [10] studied 113 patients with 354 HCC lesions from eight institutions in North America. Fifty three percent of lesions were hypointense on T1-weighted and hyperintense on T2-weighted images, 16% were isointense on both T1- and T2-weighted, 10% were hypointense on T1-weighted and isointense on T2-weighted images, 7% were hyperintense on both T1- and T2-weighted images and 6% were isointense on T1-weighted and hyperintense on T2-weighted images. Lutz et al. [11] studied 22 patients with 36 pathologically proved HCC lesions. They reported signal intensity on T1-weighted images that majority of lesions (83%) were hypointense, 11% were isointense, and 6% were hyperintense. In our study, the most common signal intensity of HCC on unenhanced T1- and T2-weighted images was hypointense on T1-weighted and hyperintense on T2-weighted images (65%), followed by hyperintense on both T1- and T2-weighted images (16%), and isointense on T1-weighted and hyperintense on T2-weighted images (10%). Atypical appearance as isointensity on T2-weighted images was observed in 9%.

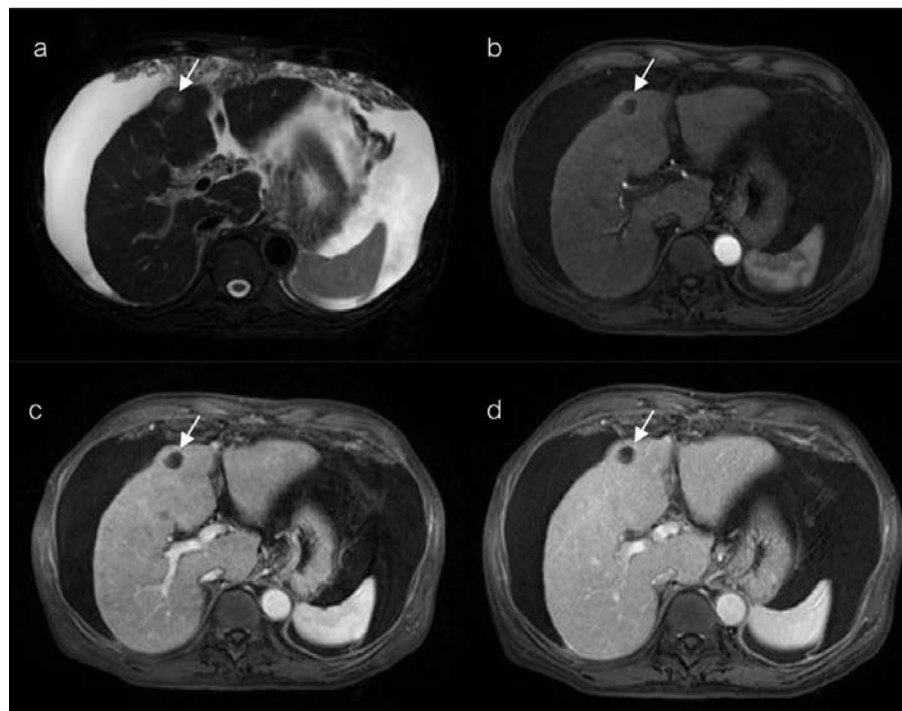


**Fig. 5** A 56-year-old man had alcoholic liver cirrhosis and a 2.2 cm HCC in the left hepatic lobe (indicated by arrows). On T2-weighted image (**a**), the nodule was mildly hyperintense. There was rim enhancement of the lesion on arterial (**b**), portovenous (**c**) and delayed phases (**d**).

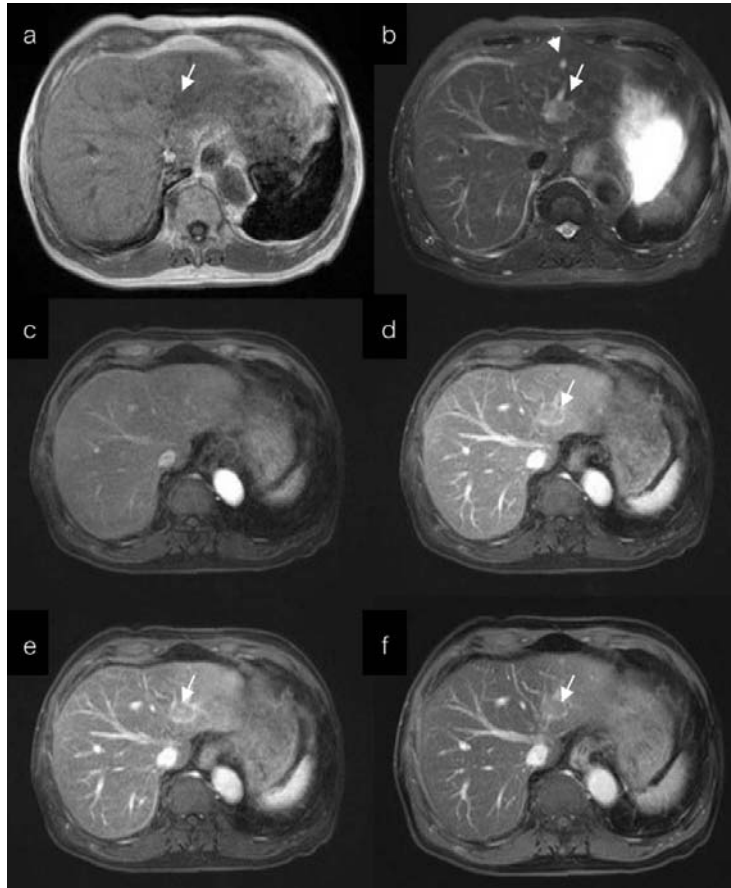


**Fig. 6** A 78-year-old man had a 2.3 cm HCC in the left hepatic lobe (indicated by arrows). This lesion was hypointense on T1-weighted (a) and mildly hyperintense on T2-weighted images (b). No enhancement was observed on the arterial phase (c). Rim enhancement was detected on the portovenous (d), equilibrium (e) and delayed phases (f). A small hemangioma was also present (indicated by arrowhead).

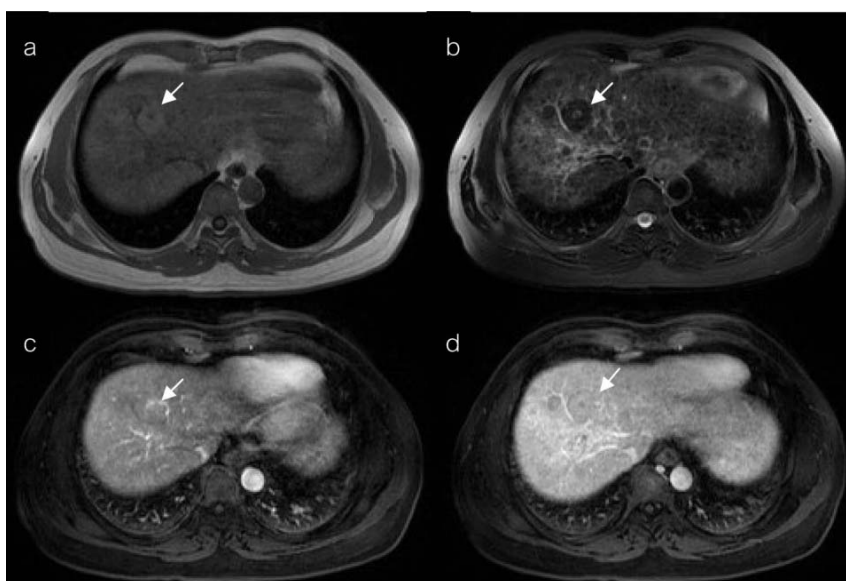


**Fig. 7** A 54-year-old man had HCC foci arising in the dysplastic nodule (indicated by arrows). T1-weighted image (a) showed hyperintense nodule with central hypointensity. On T2-weighted image (b), this nodule was hypointense with central hyperintensity. There were central enhancing foci on the arterial phase (c) which showed washout on the portovenous phase (d).

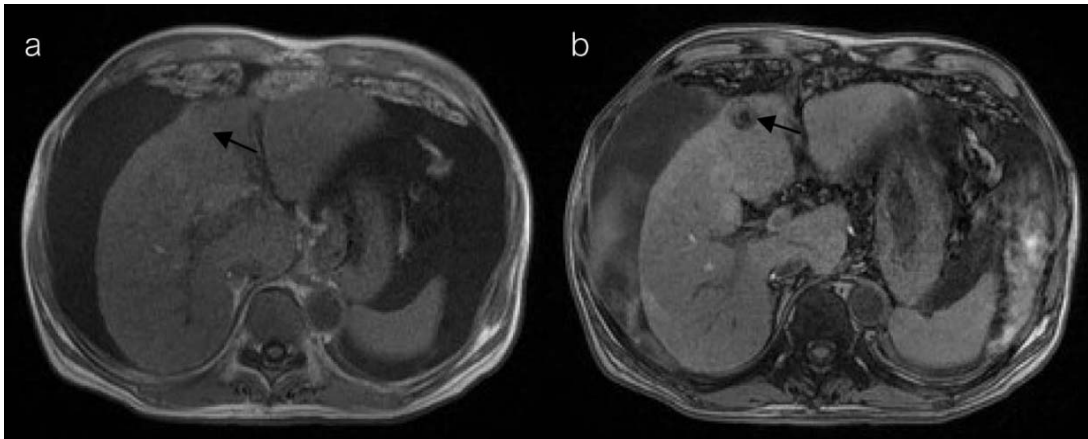


**Fig. 8** A 56-year-old man had a 2.2 cm HCC in the left hepatic lobe (indicated by arrows). The nodule showed hypointense on in phase image (a) with drop signal intensity on out-of phase image (b), representing microscopic fat component. Dynamic contrast-enhanced study of this patient was shown in Fig. 5.

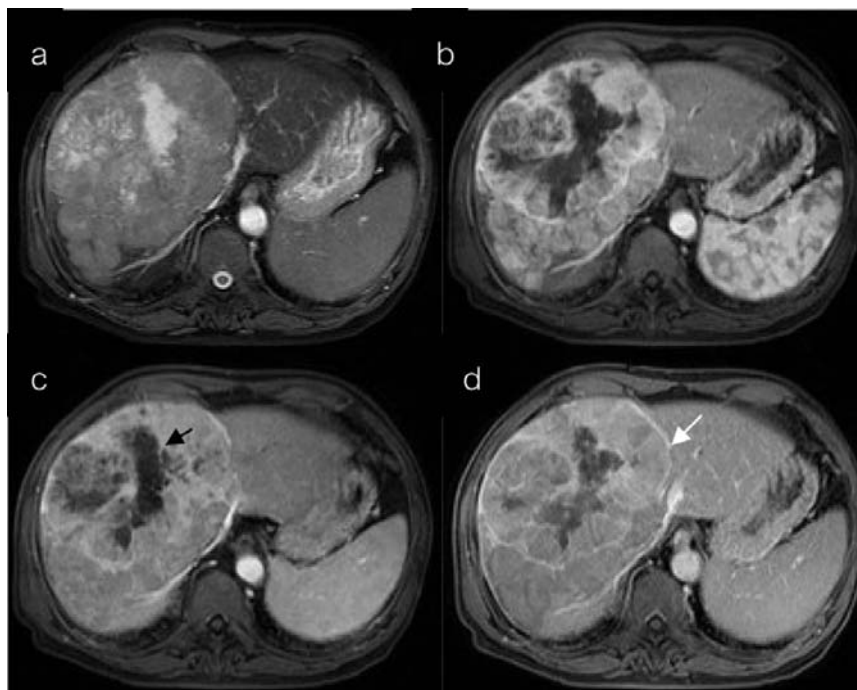


**Fig. 9** A 73-year-old man had huge HCC with central necrosis in the right hepatic lobe. This mass demonstrated mildly hyperintense with irregular markedly hyperintense center on T2-weighted image (a), heterogeneous enhancement on the arterial phase (b), washout on the portovenous phase (c) and delayed enhancing capsule on the delayed phase (d) (indicated by white arrow). Central necrosis was seen as central non-enhancement on dynamic contrast study (indicated by black arrow).

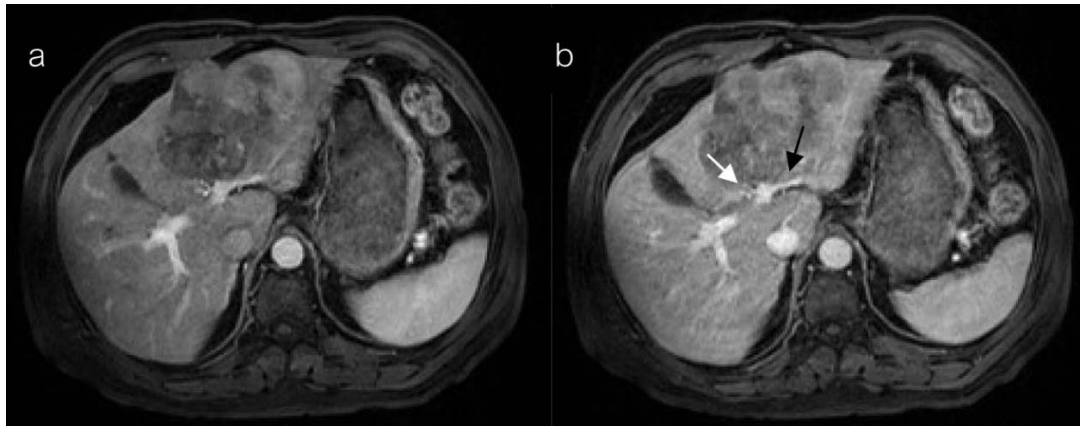


**Fig. 10** A 70-year-old man had large poorly differentiated HCC in the left hepatic lobe with portal venous invasion. On arterial phase (**a**), the lesion showed heterogeneous enhancement. On portovenous phase (**b**), the ascending branch of left portal vein was obliterated (indicated by white arrow). The horizontal branch of left portal vein was still patent (indicated by black arrow).

HCC foci arising within dysplastic nodule have characteristic “nodule within a nodule” appearance on MR imaging. On T2-weighted images, HCC appears as a small focus of high signal intensity within the low signal intensity nodule. Malignant foci show enhancement on the arterial phase after gadolinium administration. We found nodule within a nodule appearance in three lesions.

Regarding to stepwise development of HCC, there is gradual reduction of the normal hepatic arterial and portal venous supply to the nodule followed by an increase in abnormal arterial supply via newly formed abnormal arteries (neoangiogenesis) [9, 12]. This process of neoangiogenesis cause important imaging features of HCC, which is enhancement on the arterial phase. Tumors usually become hypointense on the portovenous, equilibrium and delayed phases. We found typical enhancement pattern of HCC in 84% (arterial enhancement and portovenous washout).

A minority, especially early HCC, can be isointense or hypointense on the arterial phase. This probably reflects the stage of carcinogenesis within the nodule where there has been partial or complete loss of the normal portal tract without any increased neoangiogenesis [9, 12].

In our study, HCC on the equilibrium and delayed phases were hyperintense in 21% and 19%, respectively. In the study by Lutz et al. [11], HCC lesions were hyperintense on the equilibrium phase in only 3%. Enhancement on the delayed phase of HCC may be corresponded to abundant fibrous stroma that found in scirrhous HCC [13].

Tumor capsules were identified in 62 lesions in our study. There was statistically significant relationship with large tumor size ( $p < 0.05$ ). Previous reports [7, 8, 14-17] described presence of tumor capsules in 43-90% of HCC in Asian populations and in 12-42% of HCC in non-Asian populations. Our study supported the previous reports that tumor capsules were commonly observed in Asian patients. Capsules were best detected as peripheral or rim enhancement on the delayed phase due to presence of fibrosis.

Fatty metamorphosis has been described as a specific feature of HCC on MR image. In our study, fatty metamorphosis was detected in 18 lesions (18%). Similar to the previous study in Thailand, Singcharoen et al. [17] examined 30 patients with HCC and found that presence of fatty change were noted in 20% of patients. Freeney et al. [15] reported 0% of fatty metamorphosis in 93 non-Asian patients with HCC.

Mosaic pattern of HCC produced by multiple centers of growth interspersed with areas of coagulative necrosis and/or noncancerous regenerative liver tissue [18], representing the characteristic growth pattern of HCC [19]. Kadoya et al. [7] reported overall frequency of 50%, and noted that it was more frequent in tumors larger than 3 cm (85%). Karahan et al. [16] detected 40% of the lesions had mosaic pattern. There was no statistically significant relationship between tumor size and the presence of mosaic pattern. In the study by Singcharoen et al. [17], they reported presence of mosaic pattern in 3% of cases. In this study, mosaic

pattern were detected in 42% of the lesions, and had statistically significant relationship with tumor size ( $p < 0.05$ ).

Presence of necrosis was detected in five lesions (5%) in this study. All of them were more than 2 cm in size. In the study by Kadoya et al. [7], they reported necrosis in 5% of the patients and there was statistically significant relationship between tumor size and presence of necrosis. In the study by Karahan et al. [16], necrosis was present in 33% of the tumors. The presence of necrosis showed no statistically significant relationship with tumor size and the degree of differentiation.

In our study, vascular involvement was present in six lesions (6%) and all involved the portal vein. Venous invasion was significantly related to larger tumor size more than 2 cm ( $p=0.03$ ). Previous reports [8, 15] described presence of tumor thrombus in 33-48% of patients. Stevens et al. [8] found that the frequency of venous involvement increased with increasing tumor size, where there was no statistically significant correlation between degree of differentiation and venous involvement. However, Jonas et al. [20] detected venous involvement in 40% of the cases, and found that there was statistically significant correlation between tumor size and degree of differentiation. Freeny et al. [15] described a higher incidence of venous invasion by HCC in the non-Asian populations compared with that in Asian populations.

SPIO is reticuloendothelial specific contrast agent for MR imaging of the liver. HCC typically shows high signal intensity on SPIO-enhanced T2- or T2\*-weighted images due to lack of Kupffer cells. However, some well-differentiated HCC may still contain amount of Kupffer cells, exhibiting uptake of SPIO. Vajragupta et al. [21] studied SPIO-enhanced MRI for detection of small malignant hepatic tumors. They reported SPIO could detect higher numbers of small HCC compared with gadolinium. In our study, five lesions (7%) exhibited partial SPIO. Most lesions (93%) did not uptake SPIO. SPIO was also helpful for detection and characterization of the liver tumor.

There were few limitations in our study. Firstly, most lesions had no histologically confirmation. Angiographic findings, serum  $\alpha$ -fetoprotein and other follow-up imaging were used for diagnosis of HCC in these cases. However, these modalities are accepted to be sensitive and specific for diagnosis of HCC in daily practice. Secondly, bias may have occurred in image analysis due to known diagnosis of HCC. Lastly,

the patients in this study were selected for MR imaging based on actual clinical practice. Patients with HCC, in whom CT were performed and considered to be adequate for diagnosis and treatment planning of HCC based on were not referred for MR imaging.

### Conclusion

The typical appearance of HCC was hypointense on T1-weighted, hyperintense on T2-weighted images, arterial enhancement, and portovenous washout. Mosaic pattern, necrosis, capsule, and vascular involvement were related to large HCC. Lesions with atypical appearance of HCC, for example rim enhancement or persistent enhancement on delayed phase, biopsy should be considered.

The authors have no conflict of interest to report.

### References

1. Ros PR, Erturk SM. Malignant tumors of the liver. In: Gore RM, Levine MS. *Gastrointestinal radiology*, 3<sup>rd</sup> ed. Philadelphia: Saunders Elsevier; 2008. p. 1624-33.
2. Hanna RF, Aguirre DA, Kased N, Emery SC, Peterson MR, Sirlin CB. Cirrhosis-associated hepatocellular nodules: correlation of histopathologic and MR imaging features. *Radiographics*. 2008; 28:747-69.
3. Hussain SM, Semelka RC, Mitchell DG. MR imaging of hepatocellular carcinoma. *Magn Reson Imaging Clin N Am*. 2002; 10:31-52.
4. Yamashita Y, Mitsuzaki K, Yi T, Ogata I, Nishiharu T, Urata J, et al. Small hepatocellular carcinoma in patients with chronic liver damage: prospective comparison of detection with dynamic MR imaging and helical CT of the whole liver. *Radiology*. 1996; 200:79-84.
5. Colli A, Fraquelli M, Casazza G, Massironi S, Colucci A, Conte D, et al. Accuracy of ultrasonography, spiral CT, magnetic resonance, and alpha-fetoprotein in diagnosing hepatocellular carcinoma: a systematic review. *Am J Gastroenterol*. 2006; 101:513-23.
6. Bruix J, Sherman M. Management of hepatocellular carcinoma. *Hepatology*. 2005; 42:1208-36.
7. Kadoya M, Matsui O, Takashima T, Nonomura A. Hepatocellular carcinoma: Correlation of MR imaging and histopathologic findings. *Radiology*. 1992; 183: 819-25.
8. Stevens WR, Johnson CD, Stephens DH, Batts KP. CT findings in hepatocellular carcinoma: correlation of tumor characteristics with causative factors, tumor size, and histologic tumor grade. *Radiology*. 1994; 191: 531-7.

9. Willatt JM, Hussain HK, Adusumilli S, Marrero JA. MR imaging of hepatocellular carcinoma in the cirrhotic liver: challenges and controversies. Radiology. 2008; 247:311-30.
10. Kelekis NL, Semelka RC, Worawattanakul S, Lange EE, Ascher SM, Ahn IO, et al. Hepatocellular carcinoma in North America: A multiinstitutional study of appearance on T1-weighted, T2-weighted, and serial Gadolinium-enhanced gradient-echo images. Am J Roentgenol. 1998; 170:1005-13.
11. Lutz AM, Willmann JK, Goepfert K, Marincek B, Weishaupt D. Hepatocellular carcinoma in cirrhosis: Enhancement patterns at dynamic Gadolinium- and Superparamagnetic iron oxide-enhanced T1-weighted MR imaging. Radiology. 2005; 237:520-8.
12. Matsui O. Imaging of multistep human hepatocarcinogenesis by CT during intra-arterial contrast injection. Intervirology. 2004; 47:3-5.
13. Gabata T, Matsui O, Kadoya M, Yoshikawa J, Ueda K, Kawamori Y, et al. Delayed MR imaging of the liver: correlation of delayed enhancement of hepatic tumors and pathologic appearance. Abdom Imaging. 1998; 23: 309-13.
14. Mahfouz AE, Hamm B, Wolf KJ. Dynamic gadopentetate dimeglumine-enhanced MR imaging of hepatocellular carcinoma. Eur J Radiol. 1993; 3:453-8.
15. Freeny PC, Baron RL, Teefey SA. Hepatocellular carcinoma: reduced frequency of typical findings with dynamic contrast-enhanced CT in a non-Asian population. Radiology. 1992; 182:143-8.
16. Karahan OI, Yikilmaz A, Artis T, Canoz O, Coskun A, Torun E. Contrast-enhanced dynamic magnetic resonance imaging findings of hepatocellular carcinoma and their correlation with histopathologic findings. Eur J Radiol. 2006; 57:445-52.
17. Singcharoen T, Udompanich O, Chakkapak K. Hepatocellular carcinoma: MR imaging. Australas Radiol. 1992; 36:34-6.
18. Ito K. Hepatocellular carcinoma: conventional MRI findings including gadolinium-enhanced dynamic imaging. Eur J Radiol. 2006; 58:186-99.
19. Choi BI, Lee GK, Kim ST, Han MC. Mosaic pattern of encapsulated hepatocellular carcinoma: Correlation of magnetic resonance imaging and pathology. Gastrointest Radiol. 1990; 15:238-40.
20. Jonas S, Bechstein WO, Steinmuller T, Herrmann M, Radke C, Berg T et al. Vascular invasion and histopathologic grading determine outcome after liver transplantation for hepatocellular carcinoma in cirrhosis. Hepatology. 2001; 33:1080-6.
21. Vajragupta L, Tumkosit M, Brown PL, Wangsuphachart S. Detection of small primary and secondary malignant hepatic tumors with superparamagnetic iron oxide-enhanced magnetic resonance imaging. Asian Biomed. 2008; 2:135-9.